Rapid chemical-vapor sensing using optofluidic ring resonators

Yuze Sun,[1] Siyka I. Shopova,[1] Greg Frye-Mason,[2] and Xudong Fan[1,*]

[1]*Department of Biological Engineering, 240D Bond Life Sciences Center, 1201 E. Rollins Street, University of Missouri, Columbia, Missouri 65211, USA*

[2]*ICx Nomadics, 1001 Menaul Blvd NE, Suite A, Albuquerque, New Mexico 87107, USA*

**Corresponding author: fanxud@missouri.edu*

Received February 4, 2008; revised March 1, 2008; accepted March 8, 2008; posted March 13, 2008 (Doc. ID 92417); published April 9, 2008

We develop rapid chemical-vapor sensors based on optofluidic ring resonators (OFRRs). The OFRR is a glass capillary whose circular wall supports the circulating waveguide modes (WGMs). The OFRR inner surface is coated with a vapor-sensitive polymer. The analyte and polymer interaction causes the polymer refractive index to change, which is detected as a WGM spectral shift. Owing to the excellent fluidics, the OFRR exhibits subsecond detection and recovery time with a flow rate of only 1 mL/min, a few orders of magnitude lower than that in the existing optical vapor sensors. The detection limit is estimated to be 5.6×10^{-6} refractive index units, over ten times better than other ring-resonator vapor sensors. Ethanol and hexane vapors are used as a model system, and chemical differentiation is demonstrated with different polymer coatings. © 2008 Optical Society of America

OCIS codes: 230.5750, 170.4520, 300.6320, 280.4788, 160.5470.

Optical vapor sensors have been employed in many applications, such as environmental protection, health care, and homeland security. They rely on the light intensity change or refractive index (RI) change when gas molecules are absorbed into the polymer coated on the sensor surface. Various optical structures have been investigated for RI-based vapor sensors, including waveguides, fiber Bragg gratings, surface plasmon resonance, and interferometers [1–5]. The optical ring resonator is a promising technology that can be used to develop significantly more-compact optical vapor sensors. The ring resonator supports the circulating waveguide modes (WGMs) resulting from light total internal reflection at the resonator boundaries [6]. The WGM has an evanescent field sensitive to the RI change near the resonator surface. Because of the circulating nature of the WGM, the interaction length of the WGM with the analyte can be as long as a few tens of centimeters, despite the small physical size of the ring resonator. As a result, higher light-matter interaction, hence higher sensitivity, can be achieved. Although the ring resonator has successfully been utilized for biomolecule sensing, showing a detection limit (DL) of 10^{-6}–10^{-7} refractive index units (RIU) [7,8], its potential for vapor detection has not been fully exploited. Only a handful of studies have recently been carried out on photolithographically fabricated planar ring resonators [9–11]. While a DL of tens of parts per million (ppm) has been demonstrated, these ring-resonator sensors suffer from ineffective gas fluidics, which is also commonly seen in many other optical vapor sensors. Usually, these sensors are placed in a large chamber with a gas flow rate as high as tens of liters per minute [1,5], which requires a large amount of gas samples and significantly slows down the sensing response (a few minutes to a few tens of minutes are needed [9,10]). Both tremendously deteriorate the sensor performance, especially when a fast response is needed and where only a low sample quantity is available.

In this Letter, we develop a rapid vapor sensor using an optofluidic ring resonator (OFRR) that naturally integrates the ring resonator with microfluidics. As shown in Fig. 1, the OFRR employs a thin-walled fused-silica capillary. The capillary circular wall supports the WGMs. Rather than using the outer surface for sensing, which is typical in all other ring-resonator sensors, the OFRR utilizes the optical field in the polymer layer coated on its inner surface. A thin wall is necessary to ensure sufficient light exposure in the polymer. There are a number of advantages with this type of ring resonator as a vapor sensor. First, the OFRR relies on the excellent microfluidics of a capillary, which results in rapid response time and extremely low sample volume. Second, detection can be performed at any location along the capillary. Therefore various polymers can be patterned along the capillary and respond differently to different analytes, thus enhancing the vapor-detection selectivity [1]. Third, the OFRR is highly compatible with gas chromatography (GC) that is widely used in analytical chemistry, which can be explored for micro-GC development [12]. In turn, many GC technologies, such as coating methods [13], can be adapted in OFRR vapor sensors. The OFRR has

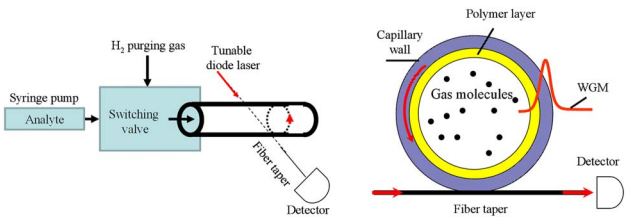

Fig. 1. (Color online) (Left) experimental setup; (right) cross-section view of the OFRR vapor sensor.

 © 2008 Optical Society of America

previously been used as a biosensor when the core is filled with liquid buffer [14]. Here, we will demonstrate another important application of the OFRR for vapor sensing. We will show that the OFRR exhibits extremely fast response even under low flow rate of only ~1 mL/min. We will further demonstrate the discriminative response of the OFRR to different vapors with different polymer coatings. Theoretical analysis will also be performed to better understand the OFRR vapor sensing performance.

Figure 1 depicts the experimental setup. The OFRR has a diameter of 75 μm and a wall thickness of approximately 4 μm [14]. The OFRR inner surface is coated with either moderately polar methyl phenol polysiloxane (OV-17, Sigma-Aldrich) or highly polar polyethylene glycol (PEG) 400 (Fluka). The coating procedures are adapted from well-developed coating procedures for GC columns [13]. The coating thickness is estimated to be approximately 200 nm for both OV-17 and PEG-400. During experiments, ethanol and hexane vapors are used to represent polar and nonpolar analytes, respectively. Various concentrations of air/analyte vapor mixture are injected into the OFRR capillary by a syringe pump at a flow rate of 1 mL/min, which is much lower than that reported in optical vapor sensors (0.1 to 10 L/min [1,5,9,10]). Ultrapure H_2 gas is applied before analyte injection to establish the sensing baseline and then after each sensing measurement to purge the analyte. A valve is used to quickly switch between the analyte and the H_2 channel. The detection part was described in detail previously [14]. In short, a 1550 nm tunable diode laser scanned in wavelength is coupled into the WGM via an optical-fiber taper or a waveguide in touch with the OFRR [14,15]. An intensity dip at the fiber output end is used to indicate the WGM spectral position. When the vapor molecules passing through the OFRR interact with the polymer, the polymer RI changes, leading to a WGM spectral shift. The Q factor of the OFRR is approximately 10^6, and the entire OFRR is placed on a plastic module covered by a glass slide to minimize temperature fluctuations.

The inset of Fig. 2(a) shows the sensorgrams when ethanol or hexane vapor is introduced to an OV-17-coated OFRR. Upon the interaction with the analyte, the WGM shifts to a longer wavelength and reaches the equilibrium value within 10 s. Then the flow is switched to H_2 to purge the OFRR, as reflected by the decrease in the WGM spectral position. There are two phenomena worthy of pointing out that attest the rapid and efficient nature of the OFRR vapor sensor. First, the purge is completed within 20 s, much faster than the previous ring-resonator designs and many other types of optical vapor sensors. Second, a thorough purge can be achieved, as evidenced by the complete return of the WGM to the baseline after purge. This is in contrast to what was previously reported in ring resonator vapor sensors, where a continuous redshift in the WGM is observed after each sensing process. Note that 10–20 s of detection time is not an intrinsic limit for the OFRR. As will be shown later, the OFRR can be operated with subsecond response time.

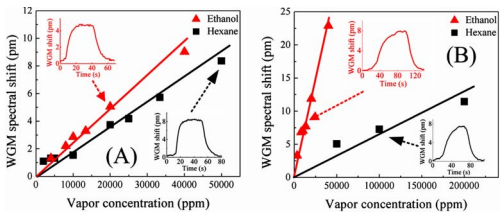

Fig. 2. (Color online) OFRR response to various concentrations of ethanol and hexane vapors. The OFRR is coated with a 200-nm-thick OV-17 (A) and PEG-400 (B). Insets are the sensorgrams taken by monitoring the WGM shift in real time.

Figure 2(a) plots the WGM shift obtained at equilibrium for various concentrations of ethanol or hexane vapor by the OV-17-coated OFRR. As expected, the sensitivity is nearly the same for ethanol and hexane, as OV-17 contains 50% polar group and 50% nonpolar group. For a comparison, Fig. 2(b) plots the sensitivity curve for ethanol and hexane using another OFRR coated with PEG-400. Both Fig. 2(a) and Fig. 2(b) indicate that the WGM shift depends linearly on the analyte concentration. Sensitivity for ethanol vapor is 0.5×10^{-3} pm/ppm, ten times higher than that for hexane, as PEG-400 is highly polar, hence having higher solubility for ethanol. To estimate the DL for ethanol vapor, we use a WGM resolution of 0.1 pm [see Fig. 3(a)], which can be obtained without any active temperature control. Based on Fig. 2(b), a DL of 200 ppm or 8 μM for ethanol vapor can be derived.

To further test the temporal response of the OFRR in vapor sensing, we replace the syringe pump with a GC injector to introduce the vapor in a pulsed manner. Figure 3 shows the subsecond response of the PEG-400-coated OFRR when ethanol or hexane vapor is introduced. The flow rate is approximately 1 mL/min. Using Fig. 2(b) as a calibration curve, the total amount of ethanol vapor used is estimated to be 30 ng. Since the OFRR sensor can resolve a WGM shift of 0.1 pm, the OFRR DL for ethanol mass is about 1 ng. As shown previously, the WGM quickly and completely returns to the baseline, indicative of thorough purge and rapid recovery for subsequent detection. Note that this response is so far limited by

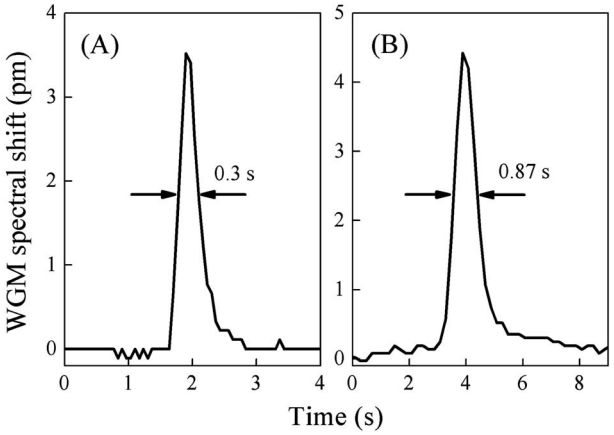

Fig. 3. Rapid detection of (A) ethanol vapor and (B) hexane vapor when the analyte is injected in a pulsed manner.

the laser scanning rate (10–15 Hz) used in our experiment. Higher detection speed is certainly possible with a higher rate.

In an optical vapor sensor, the sensing signal depends not only on the analyte solubility but also on the interaction between the analyte molecules in the polymer matrix and the WGM, which is directly related to the fraction of light in the polymer layer. To better understand the OFRR sensing capability, we carry out simulation using a four-layer Mie model, which includes the air-filled core, the polymer coating, the capillary wall, and air outside. Inset (A) in Fig. 4 shows one example of the WGM distribution when the polymer thickness is 500 nm. The corresponding WGM shift versus the polymer RI change is plotted in inset (B). Depending on the particular interaction between the polymer and the analyte, the RI change can be either positive or negative, which provides additional capability for chemical differentiation among analytes [1].

Figure 4 shows the OFRR sensitivity for various thicknesses of the polymer layer. As expected, with the increased fraction of light in the polymer, the sensitivity increases. With a 200-nm-thick coating, the sensitivity is 18 nm/RIU, corresponding to a DL of 5.6×10^{-6} RIU, which is over ten times better than reported in other ring-resonator vapor sensors [11]. The DL can be significantly improved with a thicker coating. For example, with a 1000-nm-thick polymer layer, the sensitivity becomes 160 nm/RIU, resulting in a DL of 6×10^{-7} RIU. Note that with more light in the polymer, the Q factor of the WGM will be degraded, owing to the larger optical attenuation of the polymer. However, the Q factor in excess of 10^6, and

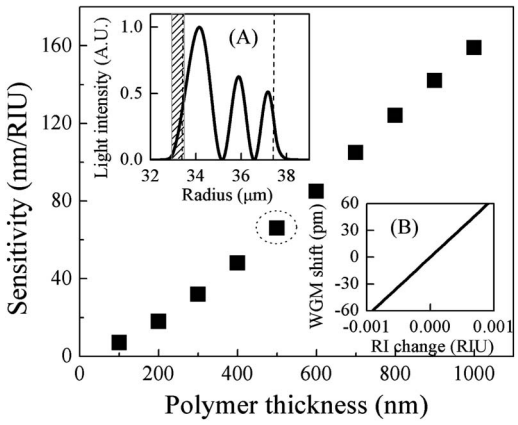

Fig. 4. Sensitivity and fraction of light in polymer versus polymer thickness. Inset (A), WGM (TE-mode) radial distribution when polymer thickness is 500 nm. Dashed lines indicate the OFRR interior and exterior surface. The shaded area represents the polymer layer. Inset (B), the corresponding WGM spectral shift as a function of the RI change in the polymer layer. OFRR outer diameter $=75\ \mu$m, OFRR wall thickness$=4\ \mu$m, core RI$=1.0$, polymer RI$=1.465$, capillary RI$=1.45$, and outside RI$=1.0$. The WGM resonant wavelength is centered around 1550 nm.

hence the 0.1 pm spectral resolution, can still be obtained with the 1000-nm-thick polymer, assuming that the polymer attenuation coefficient is 1 dB/cm.

In summary, we have developed an OFRR vapor sensor that exhibits subsecond response time with a flow rate of only 1 mL/min. Theoretical analysis shows the RI DL of the OFRR to be over ten times better than other ring-resonator technology, which can further be enhanced with a thicker polymer layer. The DL for ethanol vapor is 200 ppm in concentration or 1 ng in total mass. The OFRR vapor sensor can be employed for environmental monitoring, the battlefield, health care, and homeland security and will be particularly useful in applications where fast response is crucial.

Future work will be performed to improve the detection capability by exploring polymer-thickness-dependent sensitivity. Since a thicker polymer layer may slow down the sensor response, optimization of the OFRR will be important to investigate. Furthermore, different types of polymer will be studied to increase the analyte solubility, hence the sensitivity. Finally, patterning various polymers along the OFRR for molecule differentiation will also be pursued.

We thank Ian M. White and Aaron Thompson for helpful discussion, and we acknowledge support from the National Science Foundation (ECCS-0729903).

References

1. T. L. Lowder, J. D. Gordon, S. M. Schultz, and R. H. Selfridge, Opt. Lett. **32**, 2523 (2007).
2. H. Xiao, J. Zhang, J. Dong, M. Luo, R. Lee, and V. Romero, Opt. Lett. **30**, 1270 (2005).
3. A. Cusano, A. Iadicicco, P. Pilla, L. Contessa, S. Campopiano, A. Cutolo, M. Giordano, and G. Guerra, J. Lightwave Technol. **24**, 1776 (2006).
4. N. M. Aguirre, L. M. Pérez, J. A. Colín, and E. Buenrostro-Gonzalez, Sensors **7**, 1954 (2007).
5. J. D. Gordon, T. L. Lowder, R. H. Selfridge, and S. M. Schultz, Appl. Opt. **46**, 7805 (2007).
6. R. K. Chang and A. J. Campillo, *Optical Processes in Microcavities* (World Scientific, 1996).
7. F. Vollmer, D. Braun, A. Libchaber, M. Khoshsima, I. Teraoka, and S. Arnold, Appl. Phys. Lett. **80**, 4057 (2002).
8. N. M. Hanumegowda, C. J. Stica, B. C. Patel, I. M. White, and X. Fan, Appl. Phys. Lett. **87**, 201107 (2005).
9. A. Ksendzov, M. L. Homer, and A. M. Manfreda, Electron. Lett. **40**, 63 (2004).
10. F. Pang, X. Han, F. Chu, J. Geng, H. Cai, R. Qua, and Z. Fang, Sens. Actuators B **120**, 610 (2007).
11. V. M. N. Passaro, F. Dell'Olio, and F. D. Leonardis, Sensors **7**, 2741 (2007).
12. S. I. Shopova, I. M. White, Y. Sun, H. Zhu, X. Fan, G. Frye-Mason, A. Thompson, and S.-j. Ja, Anal. Chem. **80**, 2232 (2008).
13. S. Reidy, G. Lambertus, J. Reece, and R. Sacks, Anal. Chem. **78**, 2623 (2006).
14. I. M. White, H. Oveys, and X. Fan, Opt. Lett. **31**, 1319 (2006).
15. I. M. White, H. Oveys, X. Fan, T. L. Smith, and J. Zhang, Appl. Phys. Lett. **89**, 191106 (2006).